# AST IV inhibits $H_2O_2$-induced human umbilical vein endothelial cell apoptosis by suppressing Nox4 expression through the TGF-β1/Smad2 pathway

YUHONG MA[1,2], WEIZU LI[1], YANYAN YIN[1] and WEIPING LI[1]

[1]Department of Pharmacology, College of Basic Medicine, Anhui Medical University, Hefei, Anhui 230032; [2]Department of Diagnosis, Wannan Medical College, Wuhu, Anhui 241001, P.R. China

Received November 10, 2014; Accepted April 8, 2015

DOI: 10.3892/ijmm.2015.2188

**Abstract.** Endothelial cell apoptosis plays an important role in the pathophysiological mechanisms of vascular complications in diabetes mellitus (DM). NADPH oxidase 4 (Nox4)-dependent reactive oxygen species (ROS) aggregation is the main cause of vascular endothelial cell apoptosis. The transforming growth factor-β1 (TGF-β1)/Smad2 signaling pathway is involved in the apoptosis of several types of cells. However, the association between vascular endothelial cell apoptosis and Nox4, and the involvement of the TGF-β1/Smad2 signaling pathway in vascular endothelial cell apoptosis remain unclear. In the present study, we aimed to investigate the role of Nox4-dependent ROS production and to determine the involvement of the TGF-β1/Smad2 signaling pathway in endothelial cell apoptosis induced by oxidative stress which causes vascular injury in DM. We demonstrated that hydrogen peroxide ($H_2O_2$) increased Nox4-dependent-ROS aggregation, as well as the expression of TGF-β1, Smad2, Bax and caspase-3, decreased Bcl-2 expression and increased the apoptosis of human umbilical vein endothelial cells (HUVECs). Treatment with diphenyliodonium (DPI), a specific inhibitor of Nox4 or astragaloside IV (AST IV), a monomer located in an extract of astragaloside, decreased Nox4 expression and the levels of ROS, decreased TGF-β1 and Smad2 expression, altered the expression of apoptosis-related genes and decreased the apoptosis of HUVECs. Treatment with LY2109761, a selective inhibitor of the TGF-β1/Smad2 pathway, produced results similar to those of DPI; however, LY2109761 had no effect on Nox4 expression and ROS levels. Taken together, the findings of the present study suggest that $H_2O_2$ contributes to HUVEC apoptosis by inducing Nox4-dependent ROS aggregation and activating the TGF-β1/Smad2 signaling pathway. Our data indicate that the protective effects of AST IV against vascular endothelial cell apoptosis in DM are mainly associated with the decrease in Nox4 expression through the TGF-β1/Smad2 signaling pathway. Furthermore, the inhibition of the activation of the TGF-β1/Smad2 signaling pathway may be another potential therapeutic strategy in the treatment of DM.

*Correspondence to:* Professor Weiping Li, Department of Pharmacology, College of Basic Medicine, Anhui Medical University, 81 Meishan Road, Hefei, Anhui 230032, P.R. China
E-mail: lwp19@126.com; mayh1978@126.com

*Abbreviations:* DM, diabetes mellitus; ROS, reactive oxygen species; TGF-β1, transforming growth factor-β1; AST IV, astragaloside IV; HUVECs, human umbilical vein endothelial cells; $H_2O_2$, hydrogen peroxide; $EC_{50}$, half maximal effective concentration; MTT, 3-(4,5-dimethylthiazol-2-yl)-2,5-diphenyltetrazolium bromide; OD, optical density; $H_2$DCFDA, 2',7'-dichlorodihydrofluorescein diacetate; PBS, phosphate-buffered saline; FBS, fetal bovine serum; EDTA, ethylenediaminetetraacetic acid; qPCR, quantitative polymerase chain reaction; CT, cycle threshold; PMSF, phenylmethanesulfonyl fluoride; RT, room temperature; ANOVA, one-way analysis of variance; DPI, diphenyliodonium

*Key words:* vascular injury, diabetes mellitus, astragaloside IV, NADPH oxidase 4, reactive oxygen species, transforming growth factor-β1, Smad2, apoptosis

## Introduction

Diabetes mellitus (DM) is a complex metabolic syndrome, the prevalence of which is rapidly increasing worldwide. Among the pathophysiological mechanisms of diabetes, vascular complications are a main cause of morbidity and mortality in diabetic patients (1). Oxidative stress is the main pathophysiological mechanism of macrovascular injury and contributes to endothelial cell injury. The aggregation of reactive oxygen species (ROS) frequently damages the cytoplasm, lipids and proteins, thus resulting in vascular endothelial cell apoptosis (2-5). Cell apoptosis is the initial step in macrovascular injury and is critical to the development and progression of cardiovascular diseases (6). NADPH oxidase 4 (Nox4), a subunit of NADPH oxidase, is abundantly expressed in several types of tissue and generates free radicals in vascular endothelial cells (7,8). The inhibition of Nox4 activity has been shown to prevent adipose-derived stem cell apoptosis (9). Nevertheless, the molecular mechanisms responsible for Nox4-induced endothelial cell apoptosis remain unclear.

Transforming growth factor-β1 (TGF-β1) plays a role in the apoptosis and proliferation of a variety of cells (10-12). Smad2, a downstream cytokine of TGF-β1, is activated following the activation of TGF-β1. Activated Smad2 then translocates to

the nucleus and modulates the transcription of TGF-β1 target genes (13,14). Previous studies have demonstrated that TGF-β1/Smad2 possesses potent proliferative activity in various cell types (15-17), whereas others have demonstrated that it induces apoptosis in a number of cells (18-20). Nevertheless, to the best of our knowledge, few studies have investigated whether the TGF-β1/Smad2 pathway is involved in vascular endothelial cell apoptosis in DM.

Astragaloside IV (AST IV), which is used in traditional Chinese medicine, is a monomer located in an extract of astragaloside (Fig. 1). Our previous studies confirmed that AST IV has pharmacological effects, including anti-inflammatory and antioxidant effects in some diseases (21-23). However, to the best of our knowledge, the protective effects of AST IV against vascular injury in DM *in vitro* have not been investigated to date.

In the present study, we aimed to investigate the role of Nox4-dependent ROS production and whether the TGF-β1/Smad2 signaling pathway plays a critical role in endothelial cell apoptosis *in vitro* induced by oxidative stress, which causes vascular injury in DM, and whether AST IV inhibits hydrogen peroxide ($H_2O_2$)-induced HUVEC apoptosis by suppressing Nox4 expression through the TGF-β1/Smad2 pathway.

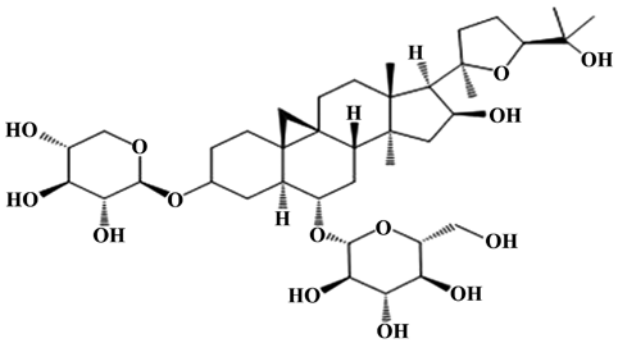


Figure 1. Structure of astragaloside IV (AST IV).

## Materials and methods

*Cell culture and administration*. Human umbilical vein endothelial cells (HUVECs; China Center for Type Culture Collection, Wuhan, China) were incubated in Dulbecco's modified Eagle's medium (DMEM) with 4.5 g/l D-glucose supplemented with 10% fetal bovine serum (FBS) (both from HyClone, Logan, UT, USA), 100 U/ml penicillin and 100 μg/ml streptomycin in a humidified atmosphere of 5% $CO_2$ at 37˚C. The HUVECs were subcultured at a 1:2 ratio interval of 2 days. Vascular injury associated with DM *in vitro* was mimicked by incubation with $H_2O_2$ 100 μmol/l for 18 h to induce damage to the HUVECs, as previously described (24). The cells were treated with each agent in the medium for 1 h prior to exposure to $H_2O_2$.

The cells were divided into 3 groups as follows: i) the control group: cells were left untreated; ii) the model group: cells were treated with $H_2O_2$ 100 μmol/l for 18 h; and iii) the AST IV group: cells were treated with AST IV for 1 h and then treated with $H_2O_2$. In addition, some cells were treated with diphenyliodonium (DPI, a specific inhibitor of Nox4; from Sigma, St. Louis, MO, USA) or LY2109761 (a selective inhibitor of TGF-β1/Smad2; from MedChem Express, LLC, Princeton, NJ, USA).

*MTT assay*. The half maximal effective concentration ($EC_{50}$) of AST IV in preventing the $H_2O_2$-induced damage to HUVECs was determined by 3-(4,5-dimethylthiazol-2-yl)-2,5-diphenyltetrazolium bromide (MTT) assay (Sigma). In brief, the cells were seeded at a density of $1x10^4$ cells/well in 96-well plates. They were then exposed to serial dilutions of AST IV in DMEM-high glucose medium and allowed to grow for the indicated periods of time. Following treatment, the cells were incubated with 100 μl DMEM-high glucose medium containing 5 mg/ml MTT. Following incubation for 4 h at 37˚C, the supernatants were discarded, MTT crystals were dissolved in 100 μl dimethyl sulfoxide (DMSO) and the optical density (OD) was measured at 570 nm using a Bio-Rad microplate reader (Bio-Rad, Hercules, CA, USA).

*ROS assay*. Intracellular ROS production was detected using a probe, the redox-sensitive fluorophore carboxy-2',7'-dichlorodihydrofluorescein diacetate ($H_2$DCFDA; Sigma) as the following steps. After delivery, the cells were washed with phosphate-buffered saline (PBS) and incubated with 20 μmol/l $H_2$DCFDA in the dark for 30 min. The cells were then briefly exposed to 0.5 g/l trypsin. The deactivation of trypsin was accomplished by the addition of PBS supplemented with 3% FBS. All cells were examined using a FACScan flow cytometer (Beckman Coulter, Miami, FL, USA) and the data were processed using FlowJo 7.6 software (Tree Star, Inc., Ashland, OR, USA) (25).

*Annexin-V and propidium iodide (PI) staining to detect apoptosis*. Following treatment, apoptosis was determined according to the following steps: the cells were collected by 0.25% ethylenediaminetetraacetic acid (EDTA)-free trypsin to digest the cells followed by centrifugation (at 1,500 rpm) to collect the cells; the cells then were suspended with 500 μl binding buffer, and the concentration was then adjusted to $1x10^6$ followed by the addition of 5 μl Annexin V-FITC staining fluid, gentle blending and incubation at 4˚C in the dark for 15 min; the cells were then treated with PI dyeing liquid at 4˚C in the dark for 5 min. Finally the cells were immediately examined using a FACScan flow cytometer (Beckman Coulter). Annexin V-FITC detection was carried out using the FL-1 and PI detection using the FL-2 channel.

*RNA extraction and reverse transcription-quantitative polymerase chain reaction (RT-qPCR)*. Total RNA was extracted using TRIzol reagent (Invitrogen, Carlsbad, CA, USA) and reverse transcribed using the First-Strand cDNA Synthesis kit (Life Technology, Carlsbad, CA, USA) according to the manufacturer's instructions. The cDNA were used as the template for the qPCR amplification using oligo primers, and the internal control for the qPCR reaction was glyceraldehyde 3-phosphate dehydrogenase (GAPDH). The primer sequences of the Nox4, TGF-β1, Smad2, Bax, Bcl-2 and caspase-3 genes (Shanghai Sangon Biotech, Shanghai, China) are presented in Table I. qPCR was performed using an ABI 7500 Real-Time PCR system (Applied Biosystems, Foster City, CA, USA). qPCR was performed with a total volume of 12 μl in each well, containing 5 μl of SYBR-Green® PCR Master Mix (Applied Biosystems), 5 μl of cDNA, and 1 μmol forward primers and 1 μmol reverse primers. Each sample was run in triplicate in a separate tube. The qPCR conditions were conducted as follows: 40 cycles of

Table I. Sequence of primers used for RT-qPCR.

| Gene | Sequence forward primer 5'→3' | Sequence reverse primer 5'→3' | Length (bp) |
|---|---|---|---|
| Nox4 | TGGACCTTTGTGCCTGTACTGT | TGAGGATGACTTATGACCGAAA | 89 |
| Smad2 | CTTTTGTTGTGTAAGCTCTCACTG | GACCTTCTACCACTTTCAGAGTTG | 243 |
| TGF-β1 | TGGACACGCAGTACAGCAAG | GCCCACGTAGTACACGATGG | 119 |
| Bax | TGGCAGCTGACATGTTTTCTGAC | TCACCCAACCACCCTGGTCTT | 195 |
| Bcl-2 | TTTGAGTTCGGTGGGGTCATG | TCACTTGTGGCTCAGATAGGC | 269 |
| Caspase-3 | AGAGGGGATCGTTGTAGAAGTC | ACAGTCCAGTTCTGTACCACG | 81 |
| GAPDH | TCCCTGAGCTGAACGGGAAG | GGAGGAGTGGGTGTCGCTGT | 217 |

qPCR, quantitative polymerase chain reaction; Nox4, NADPH oxidase 4; TGF-β1, transforming growth factor-β1; GAPDH, glyceraldehyde 3-phosphate dehydrogenase.

denaturation at 95˚C for 15 sec, annealing at 60˚C for 1 min, and extension at 72˚C for 1 min. Initial heating at 95˚C for 10 min and a final extension at 72˚C for 7 min was performed for all qPCR reactions. The cycle threshold (CT) values from all the qPCR experiments were calculated using the $2^{-\Delta\Delta CT}$ method.

*Western blot analysis*. Following treatment, the cells were lysed using RIPA buffer (Beyotime, Shanghai, China) containing 1% phenylmethanesulfonyl fluoride (PMSF; Sigma) on ice. The total protein concentrations were measured using the BCA Protein Assay kit (Beyotime). Proteins were separated by 8 or 10% SDS-PAGE and then transferred onto PVDF membranes (Millipore Corp., Billerica, MA, USA). Subsequently, the membranes were blocked with 5% non-fat milk at room temperature (RT) for 1 h, and incubated with primary antibodies as follows: anti-Nox4 (ab109225; Abcam, Cambridge, UK), anti-TGF-β1 (3712S; Cell Signaling Technology Inc., Beverly, MA, USA), anti-Smad2 (ab33875; Abcam), anti-Bax (sc-6236), anti-Bcl-2 (sc-783) (both from Santa Cruz Biotechnology, Inc., Santa Cruz, CA, USA), anti-caspase 3 (9665S; Cell Signaling Technology Inc.) and anti-β-actin (A1978; Sigma) antibodies overnight at 4˚C. Subsequently, the membranes were incubated with horseradish peroxidase-conjugated secondary anti-mouse, anti-rabbit antibodies (1:2,000 dilution) for 1 h at RT. Moreover, the proteins were visualized using an ECL advanced western blot detection kit (Pierce, Thermo, Rockford, IL, USA). Densitometric measurements of band intensity in the western blot analysis were performed using ImageJ software (National Institutes of Health, Bethesda, MD, USA).

*Statistical analysis*. All experiments were carried out 3 times. All quantified results are expressed as the means ± SEM in graphical representation. Data analysis of all results was carried out using one-way analysis of variance (ANOVA) followed by Fisher's LSD-based post-hoc analysis. All P-values were two sided and considered significant when $P<0.05$. Statistical analyses were performed with SPSS 17.0 software (SPSS, Inc., Chicago, IL, USA).

## Results

*$EC_{50}$ of AST IV in HUVECs treated with $H_2O_2$*. MTT (Sigma) assay was performed to determine the $EC_{50}$ of AST IV in inhibiting $H_2O_2$-induced damage to HUVECs. The cells were treated with AST IV at 5, 10, 25, 50, 100, 200, 400 and 800 μmol/l for 1 h prior to treatment with $H_2O_2$ and cell viability was then examined by MTT assay. The results revealed that the $EC_{50}$ of AST IV in inhibiting $H_2O_2$-induced injury to HUVECs was 100 μmol/l [calculated by regression equation (x, drug concentration; y, cell survival rate)].

*Protective effect of AST IV against $H_2O_2$-induced HUVEC apoptosis*. To assess the protective effects of AST IV against $H_2O_2$-induced HUVEC apoptosis, the mRNA and protein expression levels of Nox4, TGF-β1, Smad2, Bcl-2, Bax and caspase-3 were determined; the intercellular ROS level and the apoptotic rate were also determined. Nox4 expression in the model group was significantly increased in comparison to the control group ($P<0.01$; Fig. 2B and C). The geometric mean fluorescence intensity indicating ROS production in the control group was lower, whereas that in the model group was markedly increased ($P<0.01$; Fig. 2A). In comparison with the control group, the expression of TGF-β1/Smad2 was markedly elevated in the model group ($P<0.01$). In addition, the expression of Bax (pro-apoptotic gene) was lower and that of Bcl-2 (anti-apoptotic gene) was higher in the control group compared to the model group ($P<0.01$; Fig. 2B and C). The expression of caspase-3, a main terminal shear enzyme involved in apoptosis, was barely detectable in the control group; by contrast, its expression was upregulated in the model group ($P<0.01$; Fig. 2B and C). In comparison with the control group, the apoptotic rate was significantly increased in the model group ($P<0.01$; Fig. 2D). However, treatment with AST IV100 μmol/l reversed these effects ($P<0.01$).

*Expression of Nox4 is an important promoting event in the onset of $H_2O_2$-induced HUVEC apoptosis*. To explore the molecular mechanisms responsible for $H_2O_2$-induced HUVEC apoptosis, the HUVECs were treated with diphenyliodonium (DPI; 10 μmol, a Nox4 inhibitor) prior to treatment with $H_2O_2$. We found that treatment with DPI or AST IV decreased the expression of Nox4 (Fig. 3B and C), as well as the intercellular ROS levels in the HUVECs treated with $H_2O_2$ (Fig. 3A). Our results revealed that DPI or AST decreased TGF-β1/Smad2 expression in the HUVECs damaged by $H_2O_2$ (Fig. 3B and C). Our results also revealed that treatment with DPI or AST IV

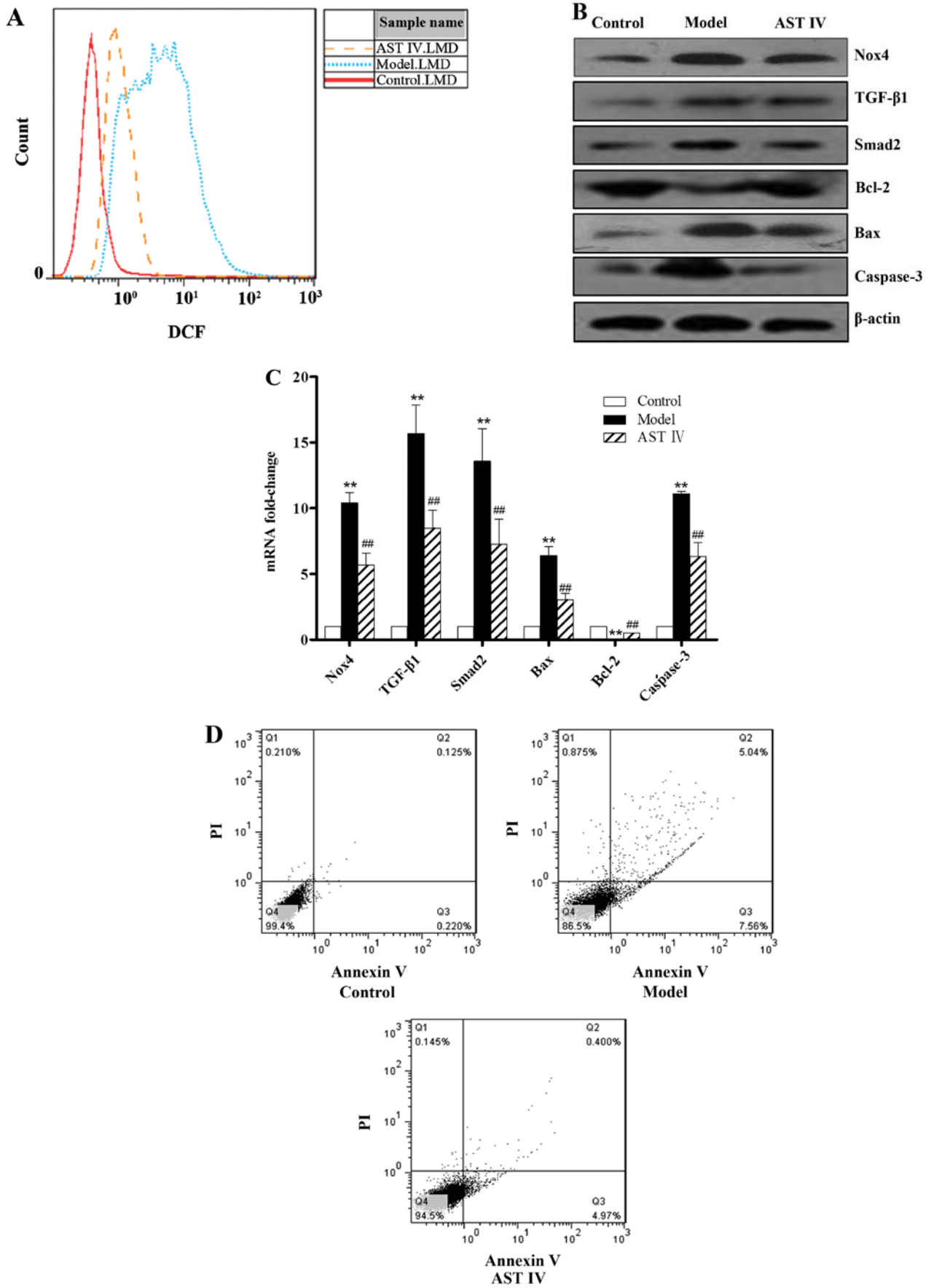


Figure 2. Protective effects of astragaloside IV (AST IV) on $H_2O_2$-induced human umbilical vein endothelial cell (HUVEC) apoptosis. (A) FACS analysis was performed to determine intercellular reactive oxygen species (ROS) levels in the HUVECs in the model, control and AST IV groups. (B) Western blot analysis was performed to determine protein expression in the HUVECs in the model, control and AST IV groups. (C) RT-qPCR was performed to determine mRNA expression in the HUVECs in the model, control and AST IV groups. (D) Annexin V-FITC/PI staining was performed to determine the apoptotic rate of the HUVECs in the model, control and AST IV groups. $^{**}$P<0.01 vs. control group; $^{\#\#}$P<0.01 vs. model group. Nox4, NADPH oxidase 4; TGF-β1, transforming growth factor-β1.

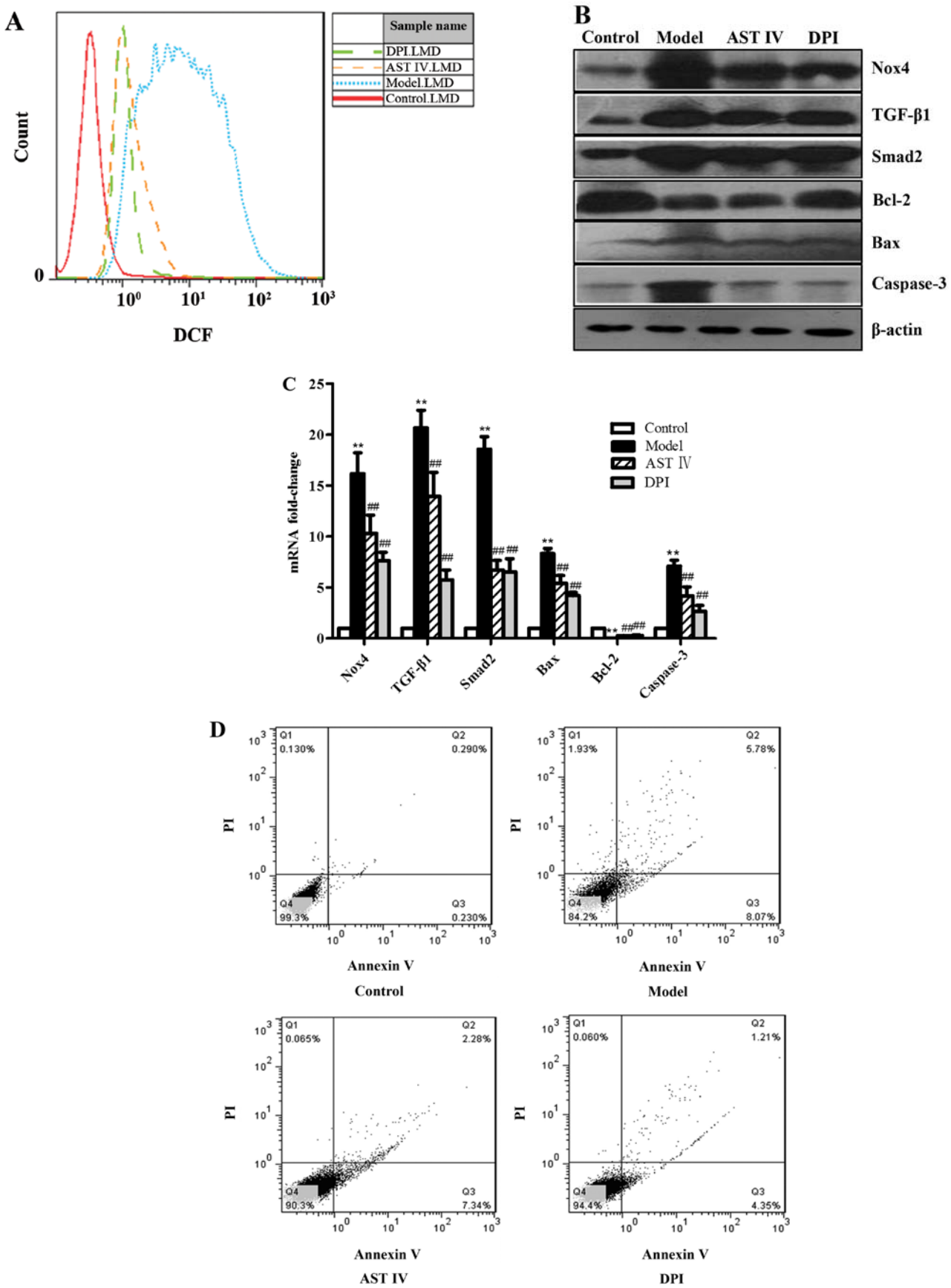


Figure 3. The overexpression of Nox4 is an important promoting event in the onset of $H_2O_2$-induced human umbilical vein endothelial cell (HUVEC) apoptosis. (A) FACS analysis was performed to determine intercellular reactive oxygen species (ROS) production in the HUVECs in the control, model, astragaloside IV (AST IV), and diphenyliodonium (DPI) groups. (B) Western blot analysis was performed to determine protein expression in the HUVECs in the control, model, AST IV and DPI groups. (C) RT-qPCR was performed to determine mRNA expression in the HUVECs in the control, model, AST IV and DPI groups. (D) Annexin V-FITC/PI staining was performed to determine the apoptotic rate of the HUVECs in the control, model, AST IV and DPI groups. $^{**}$P<0.01 vs. control group; $^{\#\#}$P<0.01 vs. model group. Nox4, NADPH oxidase 4; TGF-β1, transforming growth factor-β1.

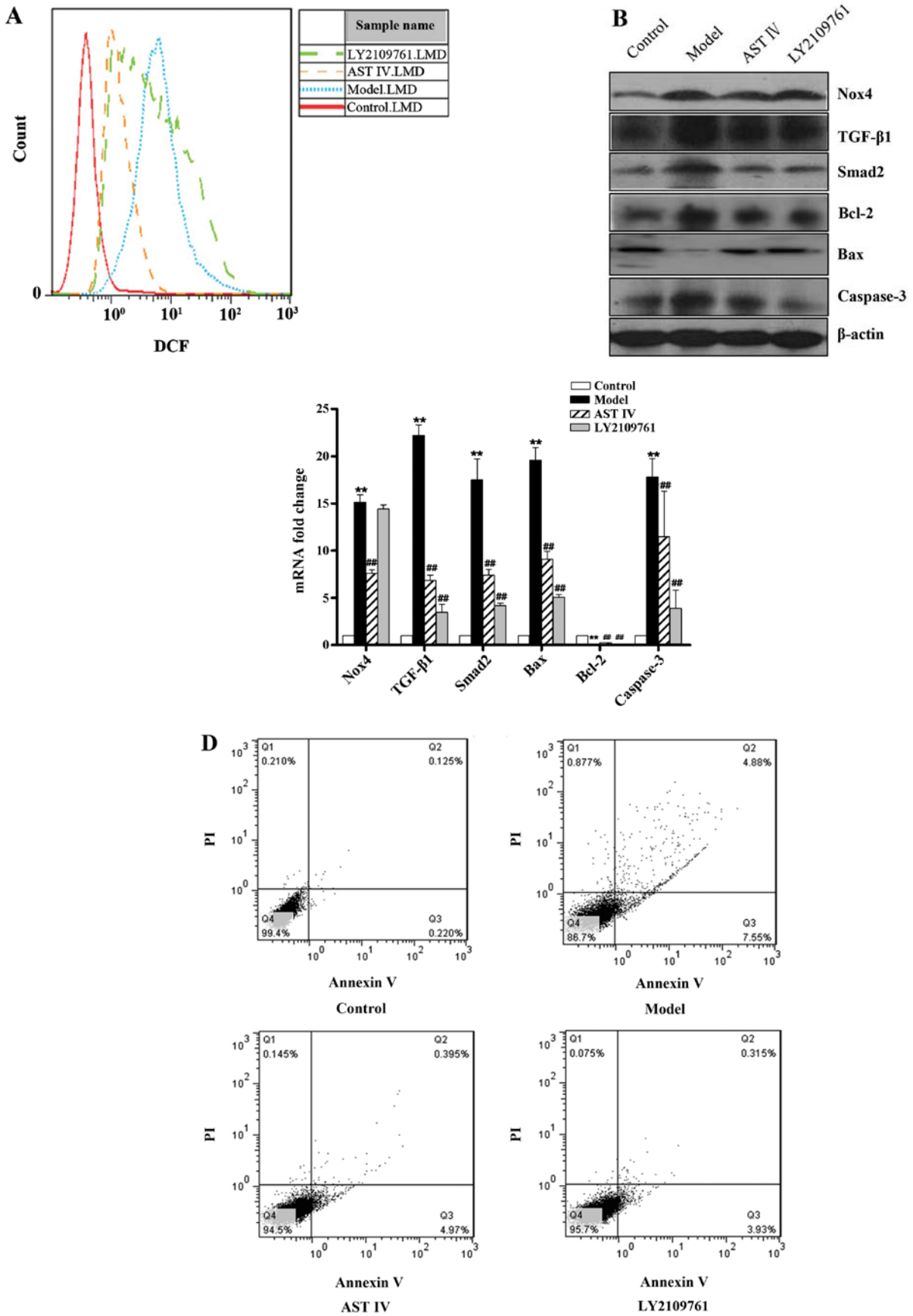


Figure 4. Inhibition of the TGF-β1/Smad2 pathway decreases $H_2O_2$-induced human umbilical vein endothelial cell (HUVEC) apoptosis, but not oxidative stress. (A) FACS analysis was performed to determine intercellular reactive oxygen species (ROS) production in the HUVECs in the control, model, astragaloside IV (AST IV) and LY2109761 groups. (B) Western blot analysis was performed to determine protein expression in the HUVECs in the control, model, AST IV and LY2109761 groups. (C) RT-qPCR was performed to determine mRNA expression in the HUVECs in the control, model, AST IV and LY2109761 groups. (D) Annexin V-FITC/PI staining was performed to determine the apoptotic rate of the HUVECs in the control, model, AST IV and LY2109761 groups. $^{**}$P<0.01 vs. control group; $^{\#\#}$P<0.01 vs. model group. Nox4, NADPH oxidase 4; TGF-β1, transforming growth factor-β1.

decreased Bax and caspase-3 expression, and increased Bcl-2 expression (Fig. 3B and C). In addition, treatment with DPI or AST IV decreased the HUVEC apoptotic rate (Fig. 3D). The exposure of the cells to AST IV at 100 $\mu$mol/l had a similar effect to that of treament with DPI (Fig. 3).

*Inhibition of the TGF-β1/Smad2 signaling pathway decreases $H_2O_2$-induced HUVEC apoptosis, but not oxidative stress*. To further investigate the role of the TGF-β1/Smad2 signaling pathway in $H_2O_2$-induced HUVEC apoptosis, LY2109761 (0.1 $\mu$mol/l), a selective inhibitor of TGF-β1/Smad2, was used to suppress the activation of the TGF-β1/Smad2 pathway. The results revealed that TGF-β1 and Smad2 mRNA and protein expression was detected at extremely low levels in the control group, whereas the overexpression of TGF-β1 and Smad2 was observed in the model group; there was a statistically significant difference between the control group and the model group ($P<0.01$; Fig. 4B and C). However, treatment with LY2109761 decreased TGF-β1 and Smad2 expression, as well as Bax and caspase-3 expression, and increased Bcl-2 expression ($P<0.01$; Fig. 4B and C). In addition, treatment with LY2109761 decreased HUVEC apoptosis ($P<0.01$; Fig. 4D), but had no effect on Nox4 expression and the ROS levels ($P>0.05$; Fig. 4A-C). Treatment with AST IV at 100 $\mu$mol/l significantly ameliorated these risk factors; it downregulated Nox4 expression (Fig. 4B and C), decreased ROS levels (Fig. 4A), decreased TGF-β1, Smad2, Bax and caspase-3 expression (Fig. 4B and C) and upregulated Bcl-2 expression (Fig. 4B and C) ($P<0.05$ and $P<0.01$ compared to model group), further decreasing HUVEC apoptosis (Fig. 4D).

## Discussion

As is known, Nox4, a subunit of NADPH oxidase, mainly catalyzes and generates intracellular ROS in vascular endothelial cells (26). The elevation of intracellular ROS production results in pathophysiological changes, including vascular inflammation in DM (27,28). This study confirmed that incubation with $H_2O_2$ at 100 $\mu$mol/l for 18 h induced Nox4 expression and ROS generation, and that the aggregation of ROS in HUVECs led to the development of endothelial cell disorders, finally resulting in vascular complications *in vitro*, as those observed in DM (28,29). On the one hand, increased ROS freely transmits the cell membrane and induces membrane lipid peroxidation and DNA damage. On the other hand, ROS augments the cell oxidative reaction system and induces cell apoptosis (30-33). In this study, following treatment with DPI, a compound which inhibits Nox4 generation, or AST IV markedly suppressed Nox4 expression, significantly decreased the generation of intracellular ROS, markedly decreased the expression of apoptosis-related genes and the apoptotic rate of the HUVECs, as demonstrated in previous studies using other agents (34-42). Therefore, the expression of Nox4 is an important promoting event in the onset of $H_2O_2$-induced HUVEC apoptosis. AST IV may thus inhibit $H_2O_2$-induced HUVEC apoptosis by suppressing Nox4 expression.

Moreover, apoptosis, or programmed cell death, is associated with the activation of multiple genes and multiple signaling pathways. The TGF-β signaling pathway is associated with oxidative stress and the apoptotic process (43-45). In this study, our results also revealed that the TGF-β1/Smad2 pathway was activated in the $H_2O_2$-treated HUVECs. TGF-β1 stimulates cell responses by signaling through the canonical Smad protein pathway, as well as using alternative pathways involving Smads, mitogen-activated protein kinases (MAPKs), protein kinase C (PKC) and phosphoinositide 3-kinase (PI3K). Activated Smad2, a downstream effector of TGF-β1 signaling, then promotes cell apoptosis (46-48). In this study, treatment with LY2109761, a selective TGF-β1/Smad2 pathway inhibitor, produced results similar to those obtained with DPI; however, LY2109761 had no effect on Nox4 expression and ROS levels. Nevertheless, AST IV decreased Nox4 expression and ROS levels, decreased TGF-β1 and Smad2 expression, decreased Bax and caspase-3 expression, and increased Bcl-2 expression and decreased HUVEC apoptosis.

Taken together, these results suggest that AST IV exerts an anti-inflammatory effect by decreasing the apoptosis of HUVECs induced by $H_2O_2$ through the inhibition of the activation of the TGF-β1/Smad2 signaling pathway. A previous study also demonstrated that AST IV possessed strong antioxidant capabilities by scavenging and neutralizing free radicals, as well as anti-inflammatory properties by inhibiting ROS formation and accumulation (23). Nevertheless, the findings of this study indicate that AST IV exerts effects similar to those of DPI, but not LY2109761. Thus, the protective effects of AST IV against vascular injury in DM *in vitro*, are mainly related to the decrease in Nox4 expression. Moreover, our results also suggest that potential therapeutic strategies to combat anti-vascular complications in DM may be developed through the manipulation of the redox status in DM. Furthermore, the inhibition of the activation of the TGF-β1/Smad2 signaling pathway may be another potential therapeutic strategy in the treatment of DM. However, the signaling pathways related to apoptosis are complex, multiple, and a number of pathways interact with each other. In this study, we only investigated the TGF-β/Smad signaling pathway; further investigations are warranted to investigate the other pathways involved. At the present time, the pharmacological effects of AST IV on vascular injury in DM need to be explored and further studies are required to determine the role of other signaling pathways.

## Acknowledgements

This study was supported by a grant form the National Natural Science Foundation of China (no. 81173624).

## References

1. Haring R, Wallaschofski H, Nauck M, Felix SB, Schmidt CO, Dörr M, Sauer S, Wilmking G and Völzke H: Total and cardiovascular disease mortality predicted by metabolic syndrome is inferior relative to its components. Exp Clin Endocrinol Diabetes 118: 685-691, 2010.
2. Erdei N, Bagi Z, Edes I, Kaley G and Koller A: $H_2O_2$ increases production of constrictor prostaglandins in smooth muscle leading to enhanced arteriolar tone in type 2 diabetic mice. Am J Physiol Heart Circ Physiol 292: H649-H656, 2007.
3. Farah R, Shurtz-Swirski R and Lapin O: Intensification of oxidative stress and inflammation in type 2 diabetes despite antihyperglycemic treatment. Cardiovasc Diabetol 7: 20, 2008.
4. Hamed S, Brenner B and Roguin A: Nitric oxide: A key factor behind the dysfunctionality of endothelial progenitor cells in diabetes mellitus type-2. Cardiovasc Res 91: 9-15, 2011.

5. Yiu KH and Tse HF: Specific role of impaired glucose metabolism and diabetes mellitus in endothelial progenitor cell characteristics and function. Arterioscler Thromb Vasc Biol 34: 1136-1143, 2014.
6. Zernecke A, Bidzhekov K, Noels H, *et al*: Delivery of microRNA-126 by apoptotic bodies induces CXCL12-dependent vascular protection. Sci Signal 2: ra81, 2009.
7. Lambeth JD: NOX enzymes and the biology of reactive oxygen. Nat Rev Immunol 4: 181-189, 2004.
8. Spillmann F, Van Linthout S, Miteva K, Lorenz M, Stangl V, Schultheiss HP and Tschöpe C: LXR agonism improves TNF-α-induced endothelial dysfunction in the absence of its cholesterol-modulating effects. Atherosclerosis 232: 1-9, 2014.
9. Scioli MG, Cervelli V, Arcuri G, Gentile P, Doldo E, Bielli A, Bonanno E and Orlandi A: High insulin-induced down-regulation of Erk-1/IGF-1R/FGFR-1 signaling is required for oxidative stress-mediated apoptosis of adipose-derived stem cells. J Cell Physiol 229: 2077-2087, 2014.
10. Camelo A, Dunmore R, Sleeman MA and Clarke DL: The epithelium in idiopathic pulmonary fibrosis: Breaking the barrier. Front Pharmacol 4: 173, 2014.
11. Herman-Edelstein M, Weinstein T and Gafter U: TGFβ1-dependent podocyte dysfunction. Curr Opin Nephrol Hypertens 22: 93-99, 2013.
12. Kamato D, Burch ML, Piva TJ, Rezaei HB, Rostam MA, Xu S, Zheng W, Little PJ and Osman N: Transforming growth factor-β signalling: Role and consequences of Smad linker region phosphorylation. Cell Signal 25: 2017-2024, 2013.
13. Blanco FF, Sanduja S, Deane NG, Blackshear PJ and Dixon DA: Transforming growth factor β regulates P-body formation through induction of the mRNA decay factor tristetraprolin. Mol Cell Biol 34: 180-195, 2014.
14. Bohanon FJ, Wang X, Ding C, Ding Y, Radhakrishnan GL, Rastellini C, Zhou J and Radhakrishnan RS: Oridonin inhibits hepatic stellate cell proliferation and fibrogenesis. J Surg Res 190: 55-63, 2014.
15. Li YC, An YS, Wang T and Zang HR: Analysis of transforming growth factor β signaling in chronic rhinosinusitis. Chin Med J (Engl) 126: 3340-3343, 2013.
16. Wang X, Chu J, Wen CJ, Fu SB, Qian YL, Wo Y, Wang C and Wang DR: Functional characterization of TRAP1-like protein involved in modulating fibrotic processes mediated by TGF-β/Smad signaling in hypertrophic scar fibroblasts. Exp Cell Res 332: 202-211, 2015.
17. Wang Z, Song Y, Tu W, He X, Lin J and Liu F: β-2 spectrin is involved in hepatocyte proliferation through the interaction of TGFβ/Smad and PI3K/AKT signalling. Liver Int 32: 1103-1111, 2012.
18. Janeesh PA and Abraham A: Robinin modulates doxorubicin-induced cardiac apoptosis by TGF-β1 signaling pathway in Sprague Dawley rats. Biomed Pharmacother 68: 989-998, 2014.
19. Liu T, Peng YF, Jia C, Yang BH, Tao X, Fang X and Zhong W: Effect of HGF on the apoptosis of rat corpus cavernosum smooth muscle cells induced by TGFβ1. Andrologia: Nov 11, 2014 (Epub ahead of print).
20. Merle P and Trepo C: Molecular mechanisms underlying hepatocellular carcinoma. Viruses 1: 852-872, 2009.
21. Li WZ, Li WP, Zhang W, Yin YY, Sun XX, Zhou SS, *et al*: Protective effect of extract of Astragalus on learning and memory impairments and neurons' apoptosis induced by glucocorticoids in 12-month-old male mice. Anat Rec (Hoboken) 294: 1003-1014, 2011.
22. Yin YY, Li WP, Gong HL, Zhu FF, Li WZ and Wu GC: Protective effect of astragaloside on focal cerebral ischemia/reperfusion injury in rats. Am J Chin Med 38: 517-527, 2010.
23. Sun L, Li W, Li W, Xiong L, Li G and Ma R: Astragaloside IV prevents damage to human mesangial cells through the inhibition of the NADPH oxidase/ROS/Akt/NF-κB pathway under high glucose conditions. Int J Mol Med 34: 167-176, 2014.
24. Ruan Y, Wu S, Zhang L, Chen G and Lai W: Retarding the senescence of human vascular endothelial cells induced by hydrogen peroxide: Effects of 17beta-estradiol ($E_2$) mediated mitochondria protection. Biogerontology 15: 367-375, 2014.
25. Wardman P: Fluorescent and luminescent probes for measurement of oxidative and nitrosative species in cells and tissues: Progress, pitfalls, and prospects. Free Radic Biol Med 43: 995-1022, 2007.
26. Yan F, Wang Y, Wu X, Peshavariya HM, Dusting GJ, Zhang M and Jiang F: Nox4 and redox signaling mediate TGF-β-induced endothelial cell apoptosis and phenotypic switch. Cell Death Dis 5: e1010, 2014.
27. Anderson TJ: Assessment and treatment of endothelial dysfunction in humans. J Am Coll Cardiol 34: 631-638, 1999.
28. Hadi HA, Carr CS and Al Suwaidi J: Endothelial dysfunction: Cardiovascular risk factors, therapy, and outcome. Vasc Health Risk Manag 1: 183-198, 2005.
29. Tousoulis D, Briasoulis A, Papageorgiou N, Tsioufis C, Tsiamis E, Toutouzas K and Stefanadis C: Oxidative stress and endothelial function: Therapeutic interventions. Recent Patents Cardiovasc Drug Discov 6: 103-114, 2011.
30. Bramlage CP, Müller GA, Tampe B, *et al*: The role of bone morphogenetic protein-5 (BMP-5) in human nephrosclerosis. J Nephrol 24: 647-655, 2011.
31. Gray SP, Di Marco E, Okabe J, *et al*: NADPH oxidase 1 plays a key role in diabetes mellitus-accelerated atherosclerosis. Circulation 127: 1888-1902, 2013.
32. Liu XQ, Sheng R and Qin ZH: The neuroprotective mechanism of brain ischemic preconditioning. Acta Pharmacol Sin 30: 1071-1080, 2009.
33. Urbański K, Nowak M and Guzik TJ: Oxidative stress and vascular function. Postepy Biochem 59: 424-431, 2013. (In Polish).
34. Dao J, Zhu L, Luo R, Hu C, Wang Y, Li H, Lu K, Liu J, Lin J and Cheng G: Molecular characterization of SjBIRP, another apoptosis inhibitor, from *Schistosoma japonicum*. Parasitol Res 113: 4065-4071, 2014.
35. Han HJ, Kwon HY, Sohn EJ, Ko H, Kim B, Jung K, Lew JH and Kim SH: Suppression of E-cadherin mediates gallotannin induced apoptosis in Hep G2 hepatocelluar carcinoma cells. Int J Biol Sci 10: 490-499, 2014.
36. Kvansakul M and Hinds MG: Structural biology of the Bcl-2 family and its mimicry by viral proteins. Cell Death Dis 4: e909, 2013.
37. Martel C, Wang Z and Brenner C: VDAC phosphorylation, a lipid sensor influencing the cell fate. Mitochondrion 19: 69-77, 2014.
38. Qiao D, Xu J, Le C, Huang E, Liu C, Qiu P, Lin Z, Xie WB and Wang H: Insulin-like growth factor binding protein 5 (IGFBP5) mediates methamphetamine-induced dopaminergic neuron apoptosis. Toxicol Lett 230: 444-453, 2014.
39. Wang G, Jiang MY, Meng Y, Song HR and Shi W: Cellular mechanisms of a new pyrazinone compound that induces apoptosis in SKOV-3 cells. Asian Pac J Cancer Prev 15: 797-802, 2014.
40. Eachkoti R, Reddy MV, Lieu YK, Cosenza SC and Reddy EP: Identification and characterisation of a novel heat shock protein 90 inhibitor ONO4140. Eur J Cancer 50: 1982-92, 2014.
41. Hou XQ, Wu DW, Zhang CX, *et al*: Bushen Yizhi formula ameliorates cognition deficits and attenuates oxidative stress related neuronal apoptosis in scopolamine induced senescence in mice. Int J Mol Med 34: 429-439, 2014.
42. Tharaheswari M, Jayachandra Reddy N, Kumar R, Varshney KC, Kannan M and Sudha Rani S: Trigonelline and diosgenin attenuate ER stress, oxidative stress-mediated damage in pancreas and enhance adipose tissue PPARγ activity in type 2 diabetic rats. Mol Cell Biochem 396: 161-174, 2014.
43. Isfort RJ, Cody DB, Stuard SB, *et al*: The combination of epidermal growth factor and transforming growth factor-beta induces novel phenotypic changes in mouse liver stem cell lines. J Cell Sci 110: 3117-3129, 1997.
44. Lee HS: Mechanisms and consequences of TGF-β overexpression by podocytes in progressive podocyte disease. Cell Tissue Res 347: 129-140, 2012.
45. Wakui H, Dejima T, Tamura K, *et al*: Activation of angiotensin II type 1 receptor-associated protein exerts an inhibitory effect on vascular hypertrophy and oxidative stress in angiotensin II-mediated hypertension. Cardiovasc Res 100: 511-519, 2013.
46. He C, Zhu H, Zhang W, Okon I, Wang Q, Li H, Le YZ and Xie Z: 7-Ketocholesterol induces autophagy in vascular smooth muscle cells through Nox4 and Atg4B. Am J Pathol 183: 626-637, 2013.
47. Li J, Li X, Xu W, Wang S, Hu Z, Zhang Q, *et al*: Antifibrotic effects of luteolin on hepatic stellate cells and liver fibrosis by targeting AKT/mTOR/p70S6K and TGFbeta/Smad signalling pathways. Liver Inter: 5 Aug, 2014 (Epub ahead of print).
48. Martínez-Palacián A, del Castillo G, Suárez-Causado A, García-Álvaro M, de Morena-Frutos D, Fernández M, Roncero C, Fabregat I, Herrera B and Sánchez A: Mouse hepatic oval cells require Met-dependent PI3K to impair TGF-β-induced oxidative stress and apoptosis. PLoS One 8: e53108, 2013.